Photosynth Res (2017) 133:357–370
DOI 10.1007/s11120-017-0376-9

ORIGINAL ARTICLE

The absence of chlorophyll *b* affects lateral mobility of photosynthetic complexes and lipids in grana membranes of Arabidopsis and barley *chlorina* mutants

Elena V. Tyutereva[1] · Anastasiia I. Evkaikina[1] · Alexandra N. Ivanova[2] · Olga V. Voitsekhovskaja[1]

Received: 8 December 2016 / Accepted: 24 March 2017 / Published online: 5 April 2017

Abstract The lateral mobility of integral components of thylakoid membranes, such as plastoquinone, xanthophylls, and pigment–protein complexes, is critical for the maintenance of efficient light harvesting, high rates of linear electron transport, and successful repair of damaged photosystem II (PSII). The packaging of the photosynthetic pigment–protein complexes in the membrane depends on their size and stereometric parameters which in turn depend on the composition of the complexes. Chlorophyll *b* (Chl*b*) is an important regulator of antenna size and composition. In this study, the lateral mobility (the mobile fraction size) of pigment–protein complexes and lipids in grana membranes was analyzed in *chlorina* mutants of Arabidopsis and barley lacking Chl*b*. In the Arabidopsis *ch1-3* mutant, diffusion of membrane lipids decreased as compared to wild-type plants, but the diffusion of photosynthetic complexes was not affected. In the barley *chlorina f2 3613* mutant, the diffusion of pigment–protein complexes significantly decreased, while the diffusion of lipids increased, as compared to wild-type plants. We propose that the size of the mobile fractions of pigment–protein complexes in grana membranes in vivo is higher than reported previously. The data are discussed in the context of the protein composition of antennae, characteristics of the plastoquinone pool, and production of reactive oxygen species in leaves of *chlorina* mutants.

✉ Olga V. Voitsekhovskaja
ovoitse@binran.ru

[1] Laboratory of Plant Ecological Physiology, Komarov Botanical Institute, Russian Academy of Sciences, ul. Professora Popova 2, 197376 Saint-Petersburg, Russia

[2] Laboratory of Plant Anatomy and Morphology, Komarov Botanical Institute, Russian Academy of Sciences, ul. Professora Popova 2, 197376 Saint-Petersburg, Russia

Keywords Chlorophyll *b* · *Chlorina* mutants · FRAP · *Hordeum vulgare* · Lateral mobility · Plastoquinone

Abbreviations

Chl	Chlorophyll
Cyt b_6/f	Cytochrome b_6/f
FRAP	Fluorescence recovery after photobleaching
LHC	Light-harvesting complex
PC	Plastocyanin
PPFR	Photosynthetic photon flux rate
PQ	Plastoquinone
PSI	Photosystem I
PSII	Photosystem II
Q_A, Q_A	Primary, secondary PSII acceptor
RC	Reaction center
ROS	Reactive oxygen species
TEM	Transmission electron microscopy
VDE	Violaxanthinde-epoxidase
WT	Wild type; the genotype with normal chlorophyll synthesis

Introduction

In terrestrial plants, composite chlorophyll *b*-containing photosynthetic antennae and a sophisticated three-dimensional organization of inner chloroplast membranes into grana evolved as adaptations to the new light environment upon the colonization of land (Kunugi et al. 2016). Chlorophyll *b* (Chl*b*), the accessory chlorophyll of land plants, has been recently revealed as a major regulator of the size and composition of photosynthetic antenna (Tanaka and Tanaka 2011). For many plant species including barley, maize, pea, rice, soybean, wheat, rape, sweet clover, cowpea, and Arabidopsis, mutants with reduced levels of Chl*b* (*chlorina*

mutants) have been described. Among them, the mutants completely lacking Chl*b* are characterized by smaller photosynthetic antennae (Bossmann et al. 1997, 1999; Takabayashi et al. 2011) and, typically, by defects in photosynthesis and productivity (Highkin and Frenkel 1962; Apel 1967; Sagromsky 1974; Tyutereva and Voitsekhovskaja 2011). The decrease in functional antennae in *chlorina* mutants leads to inefficient photoprotection and high sensitivity to light stress (Härtel et al. 1996; Leverenz et al. 1992; Lin et al. 2009; Ramel et al. 2013). Chloroplasts of these mutants usually show low degrees of grana formation (Bassi et al. 1985), probably due to the lack of the light-harvesting complex II (LHCII) which plays a role in the stacking of grana thylakoids (Standfuss et al. 2005). Thus, the reduction of antennae size in thylakoid membranes of Chl*b*-less *chlorina* mutants affects not only the function of photosynthetic complexes, but also the organization of chloroplast membranes.

Recently, the significance of the supramolecular organization of photosynthetic supercomplexes in the thylakoid membrane for the efficient functioning of the photosynthetic machinery has been elucidated (Kirchhoff 2013, 2014). The spacing of pigment–protein complexes in the membrane should allow not only efficient light harvesting but also free diffusion of electron carriers. Within the membrane bilayer, plastoquinone (PQ) should be able to cover the distance from photosystem II (PSII) to the cytochrome b_6f complex (Cyt b6/f) within several milliseconds. Also, xanthophylls should be able to move quickly within the membrane bilayer. Within the thylakoid lumen, the free diffusion of plastocyanin (PC) and violaxanthinde-epoxidase (VDE) is critical for electron transfer and zeaxanthin synthesis, respectively. Diffusion within membranes containing integral proteins follows the percolation theory (Tremmel et al. 2003; Kirchhoff 2014). Briefly, in the presence of integral membrane proteins, the apparent diffusion coefficient of a compound in the lipid bilayer depends not only on the diffusion distance but also on concentration of the proteins in the membrane. At the protein concentration defined as "percolation threshold," diffusing molecules remain "trapped" within membrane domains (Tremmel et al. 2003; Kirchhoff 2014). If, however, integral protein themselves are highly mobile and move freely within the membrane, diffusion domains do not occur. Provided the total area of protein coverage of the membrane remains constant, the larger the size of individual "obstacles" (integral membrane proteins), the less they interfere with diffusional movement of other membrane components. Thus, the formation of large supercomplexes facilitates diffusion, while at similar total coverage of the membrane with smaller complexes, the probability of collisions with protein "obstacles" increases for diffusing molecules (Tremmel et al. 2003; Kirchhoff 2014).

Kirchhoff et al. (2002) demonstrated that 60–70% of the total grana membrane area are covered with protein complexes, which is close to the percolation threshold for these membranes. In spinach, ca. 75% of grana membrane proteins are immobile at least over an observation time of several minutes, while the remaining protein fraction is highly mobile (Kirchhoff et al. 2008). Thus, the existence of diffusion domains restricting the movement of components of grana membranes is possible, and it can be expected that the size and order of supercomplexes in grana membranes will influence diffusion and all processes depending on it. The diffusion coefficient of PQ in a membrane containing integral proteins was shown to be two orders of magnitude lower than in liposomes, and the speed of diffusion of PQ is likely to be a limiting step in its oxidation by Cyt b_6/f (Blackwell et al. 1994). The lack of free equilibration between the reduced and the oxidized PQ pool indirectly points to the presence of diffusion domains for PQ in grana membrane (Lavergne et al. 1992; Kirchhoff et al. 2000). The existence of nanodomains harboring PSII and Cyt b_6/f in spinach grana membrane has been demonstrated; they were suggested to be functional equivalents of PQ diffusion domains (Johnson et al. 2014).

At the same time, membrane components of the photosynthetic apparatus should be positioned close enough to allow quick and efficient transfer of energy and electrons, but not too close as to avoid the generation of unnecessary quenching aggregates of the LHC proteins. Haferkamp et al. (2010) demonstrated that the fusion of isolated granal membranes with liposomes caused a "dilution" of pigment–protein complexes with lipids which influenced functional connection between PSII and LHCII. This study revealed that an "optimal" density of protein complexes in the membrane exists, i.e., a density which allows optimal photosynthetic activity. Apart from this aspect, the lateral mobility of pigment–protein complexes in grana membranes is critically important for the regulation of light harvesting which occurs via shuttling of LHCII between PSII and PSI and for the PSII repair cycle (Kirchhoff 2014). Of all pigment–protein complexes, PSII, and within the PSII, the D1 protein in particular, is sensitive to damage by excess light at the highest degree, and the efficient repair of D1 is crucial for photosynthesis to avoid photoinhibition (Allakhverdiev and Murata 2004; Nishiyama et al. 2005; Murata et al. 2007). The unchallenged lateral mobility of membrane components is a prerequisite for this repair (Kirchhoff 2014).

The lateral mobility of membrane components also depends on the fluidity of membranes which is directly related to the degree of unsaturation of membrane lipids (reviewed in Los et al. 2013). The role of unsaturated thylakoid lipids in prevention of the inhibition of photosynthesis during various stresses via facilitation of the recovery

of PS II has been reviewed by Kreslavski et al. (2007). The degree of saturation of thylakoid lipids, especially of phosphatidylglycerols, is a very important parameter for the proper functioning of not only PSII but also PSI: a genetically introduced decrease in the amount of unsaturated phosphatidylglycerols in thylakoid membranes resulted in strong photoinhibition of PSI at high light (Ivanov et al. 2012). It can be concluded that both the lipid composition of thylakoid membranes and the proportion of unsaturated lipids in the membranes are of great significance for the proper functioning of photosynthesis.

As the size of PSII supercomplexes depends on the composition and number of attached antennae, it can be expected that the spacing of pigment–protein complexes in *chlorina* mutants lacking Chl*b* will be altered compared to wild-type (WT) plants due to the smaller size of antennae in the former. Generally, the reduction in LHCII size in *chlorina* mutants is more severe than for LHCI and/or for the minor antenna (Bossmann et al. 1997, 1999; Takabayashi et al. 2011), but the composition of PSII antenna is affected to different extents depending on the mutant. Study by Goral et al. (2012) performed with several lines of transgenic Arabidopsis plants demonstrated that the absence of individual Lhcb proteins had different effects on the mobility of chlorophyll-containing proteins in granal membranes. As shown by studies on Arabidopsis Lhcb6 knockout lines, these plants formed smaller PSII supercomplexes and displayed impaired diffusion of PQ, impaired electron transport, and other functional defects which the authors related solely to the changed supramolecular organization of grana membranes (de Bianchi et al. 2008). In the present study, we addressed the question whether and how lateral mobility of pigment–protein complexes and membrane lipids is affected in two mutants with the altered composition of antennae, barley *chlorina f2 3613* (*clo f2*^{3613}), and Arabidopsis *ch1-3*, respectively. Both mutants are lacking chlorophyllide-a-oxygenase (CAO) and therefore are completely devoid of Chl*b* (Espineda et al. 1999; Mueller et al. 2012). In these mutants, we determined the sizes of the mobile fractions of chlorophyll-containing proteins and lipids, respectively, and compared them to those in the WT. We further addressed the question whether altered lateral mobility of proteins and lipids might affect the redox dynamics of the PQ pool in barley *clo f2*^{3613} and Arabidopsis *ch1-3* mutants.

Materials and methods

Plant growth

Seeds of *Arabidopsis* lines (*Col-0* and *ch1-3*) were obtained from the Nottingham Arabidopsis Stock Centre. Seeds of the *Hordeum vulgare* mutant *chlorina* 3613 (*clo f2*^{3613}) and of the parent cultivar Donaria were obtained from the Leibniz Institute for Plant Genetics and Crop Plant Research (Gatersleben, Germany). Arabidopsis seeds were germinated on MS (Murashige and Skoog 1962) agar containing 2% sucrose and transferred to garden soil. Both lines, *Col-0* and *ch1*-3, were grown at 22 °C with a PPFR of 130 µmol m^{-2} s^{-1} in an 8-h light/16-h dark cycle for 5 weeks and then transferred to a 16-h light/8-h dark cycle. *Col-0* plants were 6–7 weeks old when taken for analyses. *Ch1-3* plants which display delayed development were analyzed 8–10 weeks after germination, when their leaves were approximately of the same size as the leaves of WT plants at 6 weeks. Barley plants used for electron microscopic studies were cultivated outdoors on a plot belonging to the Komarov Botanical Institute RAS from May to September in 2014 and 2015. Leaves of 3- to 4-week-old plants were fixed for transmission electron microscopy as described below. Barley plants for all other studies were grown in a greenhouse during September to November under regular watering and combined natural sun and artificial light under a 16-h light/8-h dark cycle at 19–23 °C. Leaves of 3- to 6-week-old plants were used for experiments.

Isolation of chloroplasts and photochemically active thylakoid membranes and preparation of samples for fluorescence recovery after photobleaching (FRAP) analyses

Intact chloroplasts were isolated as described in Whitehouse and Moore (1993) with some modifications. All steps were performed at 4 °C using precooled glassware. Leaves (1.5 g) were cut off the plants, cooled in ice-cold water, and grounded in cold buffer #1 containing 330 mM sorbitol, 50 mM HEPES-KOH pH 6.5, 5 mM $MgCl_2$, 0.1% (w/v) NaCl, and 0.1% (w/v) BSA. Note that *iso*-ascorbate was omitted from the buffer, as it would interfere with the fluorescence analyses of BODIPY (our observations; Dulin et al. 2010). The extracts were centrifuged for 5 min at 4500 rpm; the pellets were resuspended in buffer #2 containing 330 mM sorbitol, 50 mM HEPES-KOH pH 7.6, 2 mM EDTA, 1 mM $MgCl_2$, and 1 mM $MnCl_2$. The intactness of chloroplasts was estimated by ferricyanide reduction (Whitehouse and Moore 1993): only chloroplast suspensions with intactness >60% were used. To obtain the fraction of thylakoid membranes, isolated chloroplasts were sedimented by centrifugation for 5 min at 4500 rpm and resuspended in shock medium containing 15 mM NaCl, 5 mM $MgCl_2$, and 20 mM HEPES-KOH pH 7.5. The shocked chloroplasts were then washed three times with buffer #2 followed by pelleting for 5 min at 4500 rpm, and then resuspended in a small volume of buffer #3 containing 330 mM sorbitol, 20 mM HEPES-KOH pH 7.5, 15 mM

NaCl, and 5 mM $MgCl_2$. The concentration of chlorophyll in the suspension was determined according to Arnon (1949).

For FRAP measurements, suspensions of chloroplasts or of thylakoid membranes were used with a concentration of total chlorophyll of 1 mg ml^{-1}. Immobilization of chloroplasts was performed as follows. 60 µl of poly-L-lysin (0.1% in water) were pipetted onto a glass slide; 60 µl of chloroplast suspension were added; after 5-min incubation, the liquid was carefully removed from the slides using filter paper. 120 µl of buffer #2 were then pipetted onto the immobilized chloroplasts and then removed from the slides using filter paper. The chloroplasts in residual buffer #2 were covered with a cover slip and used for FRAP analyses. Diffusion of pigment–protein complexes was analyzed using recovery of chlorophyll fluorescence. Diffusion of thylakoid membrane lipids was estimated using the fluorescence recovery of a fluorescent fatty acid analog C1-BODIPY FL C12 500/510 (4,4-difluoro-5-methyl-4-bora-3a,4a-diaza-s-indacene-3-dodecanoic acid; Thermo Fisher Scientific, USA). For chlorophyll FRAP analysis, only chloroplasts with intact outer envelope (as visualized by BODIPY staining) were used. BODIPY has an emission peak at 512 nm and a C12 fatty acid tail. For incorporation of the BODIPY into membranes, suspensions of chloroplasts or of thylakoid membranes were incubated in buffer #2 with BODIPY added to a final concentration of 1 µM for 10 min and then repeatedly washed with buffer #2 without BODIPY as described above. The chloroplasts in residing buffer #2 were coated with a cover slip and used for FRAP analyses.

FRAP measurements and analysis

FRAP experiments were performed using laser scanning confocal system LSM 780 (Carl Zeiss, Germany). Fluorescence was excited using lines of 633 nm (He–Ne laser) and of 488 nm (argon laser at 100 mW) for chlorophyll (Chl) and BODIPY, respectively. Emitted fluorescence was collected in the 665–720 nm region and in the 500–527 nm region for Chl and BODIPY, respectively. On a selected patch of thylakoid membrane, fluorescence of Chl or of BODIPY was bleached down to 50% of the initial level with short laser pulses of 100% power at 405 nm for Chl and at 488 for BODIPY, respectively. During the experiment, fluorescence emission was collected simultaneously from three regions of interests (ROI): (a) bleached patch of the thylakoid membrane, (b) reference (non-bleached) patch of the thylakoid membrane, and (c) background region outside the thylakoid membrane. Data on fluorescence intensities and images analyses were evaluated using Zen 2.1 software (Carl Zeiss) and the Excel 2010 statistical package.

The size of the mobile fraction (R) was calculated according to Reits and Neefjes (2001) using the formula $R=(F_\infty-F_0)/(F_i-F_0)$, where F_∞ is the fluorescence in the bleached region after full recovery, F_0 is the fluorescence just after bleaching (at time t_0), and F_i is the fluorescence before bleaching. Corrections were introduced for background fluorescence, the F_0 values were normalized to zero, and the curves of fluorescence recovery after photobleaching were constructed for thylakoid membranes of chloroplasts isolated from leaves of wild type and *chlorina* mutants of Arabidopsis and barley.

Fluorescence measurements

Chl*a* fluorescence of leaves of light-adapted plants of barley and Arabidopsis was measured at a growth temperature of 20 °C under ambient CO_2 conditions using a Portable Chlorophyll Fluorometer PAM-2500 (Heinz Walz GmbH, Effeltrich, Germany). The state of oxidation of the PQ pool in the light in intact leaves was calculated as $1-qL$, where $qL=(F'_m-F_s)/(F'_m-F'_o)$ (Kramer et al. 2004; Borisova-Mubarakshina et al. 2015); F'_o is the minimum yield of Chl fluorescence immediately after the cessation of illumination; F_s is the steady-state fluorescence at light, and F'_m is the maximum fluorescence emitted from a light-adapted leaf. Maximal fluorescence F'_m was measured using saturating pulses (8000 µmol m^{-2} s^{-1} PAR, 100-ms duration). Leaves adapted to the growth light (4 h, 150 µmol m^{-2} s^{-1} PAR for Arabidopsis and 800 µmol m^{-2} s^{-1} PAR for barley) were fixed by leaf clip and additionally lightened by internal PAM red lamp for 5–10 min (light intensity 1000 µmol m^{-2} s^{-1} PAR for Arabidopsis and 1500 µmol m^{-2} s^{-1} PAR for barley, respectively; total actinic light level was controlled by internal leaf clip quantum meter) until the reaching of steady-state F_s level. Then the leaves were exposed to darkness, and the Chl fluorescence was measured immediately after the cessation of the light. Polyphasic Chl*a* fluorescence transient measurements (O–J–I–P measurements) of leaves of dark-adapted plants (kept in darkness for 10 h before analysis) were performed with the same system using saturating red light and 300-ms polyphasic fluorescence trigger mode. The size of the total (reduced) PQ pool was determined as the area above the O–J–I–P curve (between F_o and F_m and the F_m asymptote) for leaves poisoned with 200 µM of DCMU (Strasser et al. 2000, 2004; Kalaji et al. 2014). ET_{2o}/RC (representing quantum yield of electron transport from Q_A to Q_B in PSII) was calculated as $ET_{2o}/RC=(1-F_0/F_m)(1-V_j)$, where $V_j=(F_{2ms}-F_0)/(F_m-F_0)$ is relative variable fluorescence at time 2 ms after start of actinic light pulse (Brestic and Zivcak 2013). ABS/RC [representing the flux of absorbed photon energy (ABS) per active PSII reaction center (RC)] was calculated as $ABS/RC=M_0(1/V_j)(1/(1-F_0/F_m))$, where

M_0 is the initial slope of relative variable Chl fluorescence (Brestic and Zivcak 2013). The data were analyzed using PamWin V3.20w4 software. Functional PSII antenna size was estimated as the reciprocal of the time corresponding to 2/3 of the maximal chlorophyll fluorescence intensity for DCMU-poisoned leaves (Havaux et al. 2007). Briefly, detached leaves from dark-adapted (8 h) plants were infiltrated with 200 µM DCMU in 150 mM sorbitol and put on wet paper for 1 h in the dark before the O–J–I–P transient measurements.

Protein extraction and blotting

All steps of extraction were performed on ice using prechilled glassware. Leaf tissues (100–150 mg) were frozen in liquid nitrogen, ground to a fine powder in a mortar with a pestle, and transferred to 2-ml Eppendorf tubes. The extraction buffer consisted of 50 mM Tris–HCl pH 8.0, 5 mM $MgCl_2$, 1 mM PMSF, and protease inhibitor cocktail (cOmplete Mini, Roche). 1 ml of cold extraction buffer was added to each tube; samples were kept on ice until thawing and vortexed every 30 s. The mixtures were centrifuged for 10 min at 14,500×g at 4 °C. The supernatants were decanted, and the pellets were resuspended in 1 ml cold extraction buffer. After centrifugation under the same conditions, the pellets were washed with 1.5 ml of 80% acetone. Then the mixtures were sonicated for 10 min (Elma-Sonic S10, Germany) and centrifuged again under the same conditions. The pellets were resuspended in 200 µl of sample buffer each [150 mM Tris–HCl pH 8.0, 6% lithium dodecyl-sulfate (LDS), (Sigma-Aldrich), 150 mM DTT, 30% v/v glycerol] and boiled at 95 °C for 5 min. Extracts were stored at −80 °C.

Extracts of membrane proteins obtained as described above were separated on 12% (w/v) SDS–polyacrylamide gels. After electrophoresis, the polypeptides were transferred to a polyvinylidene difluoride membrane (Bio-Rad Laboratories, USA), and the membrane was blocked with 2.5% (w/v) Blotto Non-Fat Dry Milk (Santa Cruz Biotechnology, USA) overnight. Blots were incubated with the primary antibody diluted according to manufacturer's instructions for 1.5 h at room temperature with agitation. Primary antibodies to PsbA, PsaB, Lhcb1, Lhcb2, Lhcb3, Lhcb4, Lhcb5, Lhcb6, Lhca1, Lhca2, Lhca3, Lhca4, and PetA were provided by Agrisera (Sweden). The antibody solution was decanted and the blot was washed three times for 5 min in TBS-T buffer (50 mM Tris pH 7.5, 150 mM NaCl, 0.1% Tween 20) at room temperature with agitation. Blots were incubated in secondary antibody (anti-rabbit IgG HRP conjugated secondary antibody, Agrisera, Sweden) diluted 1:25,000. Signal was detected after incubation of blots in West Dura working solution (SuperSignal West Dura Extended Duration Substrate, ThermoScientific, USA) for 1–15 min and exposure to Fuji medical X-ray film (Super RX, Japan).

For semi-quantitative estimation of relative amounts of PetA and PsbA proteins, blots were run with three different dilutions of protein extracts. Time intervals for film exposures were selected as to avoid under- or overexposure of the blots. Quantitation of the relative intensities of bands was performed using ImageJ 1.37v software (NIH, USA).

Fluorescence microscopy

Levels of reactive oxygen species (ROS) were examined in leaves of barley (WT and *clo f2*^{3613}) using ROS-specific fluorescent probes (Schmitt et al. 2014): the chloromethyl derivative of 2′,7′-dichlorodihydrofluorescein diacetate, CM-H_2DCFDA (Molecular Probes, USA), or singlet oxygen sensor green (SOSG) (Molecular Probes, USA). Detached leaves were infiltrated either with CM-H_2DCFDA or with SOSG dissolved at a concentration of 5 µM of each dye in a buffer containing 50 mM KCl, 10 µM $CaCl_2$, and 10 mM MES, pH 6.15, and then exposed to light for 2 h (using a sodium light source yielding 1500 µmol photons m^{-2} s^{-1}). The leaves were observed using a BX51 epifluorescence microscope (Olympus Deutschland GmbH, Hamburg, Germany) equipped with a BP 460–490, DM 505, BA 510–550 filter. Images were captured using a ColorView II digital camera and Cell^F software (Olympus). Relative intensities of ROS staining were estimated using ImageJ 1.37v software (NIH, USA).

Electron microscopy of isolated grana membranes

Grana membranes were isolated according to Morosinotto et al. (2006), with some modifications, using 5 g of barley leaves (WT or *clo f2*^{3613}, respectively) for each isolation. The method of sequential droplets was used for the negative stain procedure. Carbon-coated copper 300 mesh grids were placed upon the drops of suspension and left for 1 min to absorb grana membranes on the grid surface. Then, the specimens were fixed with 0.5% glutaraldehyde in a buffer containing 20 mM HEPES pH 7.5, 0.4 M sorbitol, 15 mM NaCl, and 5 mM $MgCl_2$ for 30–60 s, washed several times with water and negatively stained with 1% uranyl acetate solution in water. Transmission electron microscopy was performed at 120 kV using a Libra 120 plus electron microscope (Carl Zeiss) equipped with a BM-2k-120 dual-speed on axis SSCCD camera (TRS, Germany).

Statistics

The means of five replicates and their standard deviations are shown. Reliability of differences between the mean values was estimated using Student's *t* test at a significance

level of 95%. Significance of differences between the curves shown in Fig. 1 was estimated using one-way ANOVA.

Results

Lateral mobility of chlorophyll-containing proteins and lipids is differently affected by the CAO mutation in barley and Arabidopsis

Chl fluorescence (monitored by excitation of intact chloroplasts with a low-intensity red laser) was bleached by a high-intensity ultra-violet laser in a small region (stripe) in chloroplasts of barley and Arabidopsis leaves (WT and *chlorina* mutants), and the recovery was observed over several minutes (Fig. 1a). In another series of experiments, fluorescence of thylakoid membranes stained with BODIPY was monitored by excitation with a low-intensity blue laser and bleached using the same laser at high intensity (Fig. 1b). Chl fluorescence of intact isolated chloroplasts represents mainly the fluorescence of LHCII and PSII, while BODIPY fluorescence after its incorporation into thylakoid membranes can be used to estimate lipid diffusion (Tietz et al. 2015). The intactness of chloroplasts was estimated based on the uniformity of staining of the outer envelope with BODIPY (Fig. 1c). Analyses of the recovery curves showed that Chl fluorescence in WT barley recovered faster than in barley *clo f2*^{3613} (Fig. 1d, e). The size of the mobile fraction (i.e., the fraction of fluorescence that recovers in FRAP experiments) was significantly lower in barley *clo f2*^{3613} than in WT. In Arabidopsis, no significant differences in the rate of Chl fluorescence recovery, and thus in mobile fractions, were found between WT and *ch1-3* mutant (Fig. 1f, g). Analyses of the recovery curves for BODIPY fluorescence revealed significant differences in the rates of recovery, and thus in the size of the mobile fraction of fluorescence, between barley WT and *clo f2*^{3613} (Fig. 1h, i). The mobility of BODIPY was significantly higher in the membranes of barley *clo f2*^{3613} than in WT

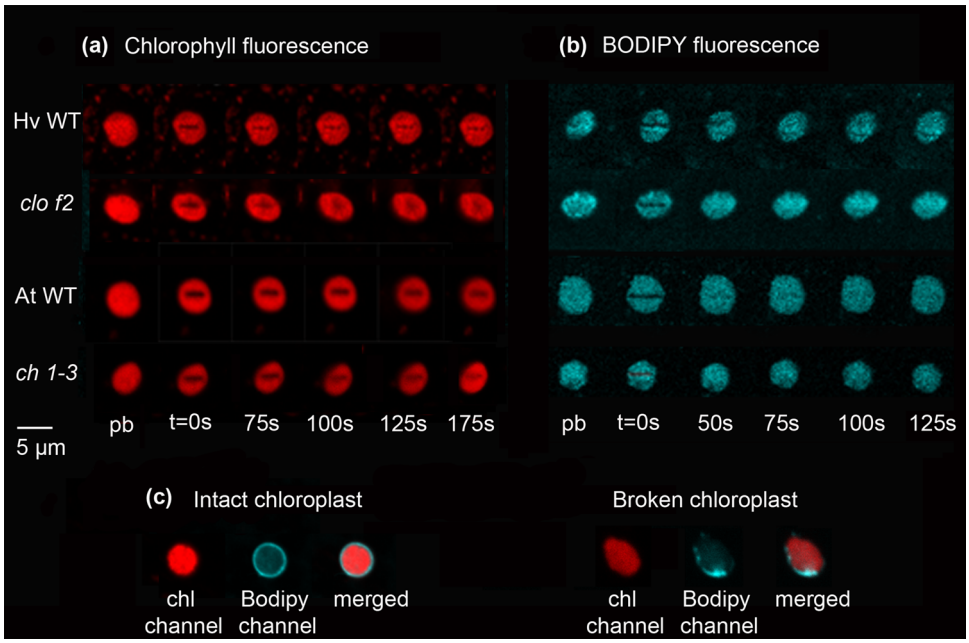

Fig. 1 FRAP analysis on isolated chloroplasts and thylakoid membranes of Arabidopsis (At) and barley (Hv) WT and *chlorina* mutants (*ch1-3* and *clo f2*^{3613}, respectively): **a, b** examples for Chl (**a**) and BODIPY fluorescence (**b**) time series. The line bleach was induced at time point zero ($t=0$ s); *pb* prebleach images. Chl fluorescence of intact isolated chloroplasts was used to estimate mainly the mobility of LHCII and PSII, while BODIPY fluorescence of thylakoid membranes was used to estimate lipid diffusion. Note that Chl fluorescence recovery is slowed down in the barley *clo f2*^{3613} mutant relative to WT barley. Note the faster recovery of BODIPY fluorescence in barley *clo f2*^{3613} mutant and the slower recovery in Arabidopsis *ch1-3* mutant as compared to corresponding WTs. **c** Example of an intact isolated chloroplast used for FRAP analyses. *Red* channel shows Chl fluorescence and *blue* channel shows BODIPY fluorescence. Note the intactness of the outer membrane uniformly stained with BODIPY. **d–k** Statistical analysis of the FRAP data for Chl fluorescence (**d–g**) and BODIPY fluorescence (**h–k**) for barley WT (**d, h**), barley *clo f2*^{3613} (**e, i**), Arabidopsis WT (**f, j**), and Arabidopsis *ch1-3* (**g, k**). Chl or BODIPY were bleached at time point zero (corresponds to $t=0$ s in **a, b**). Each graph shows several curves representing independent experiments (5–6 for each variant). The percent values give the mobile fraction that recover in the course of the experiment. Parameters of the curves on **d–k** were compared using ANOVA. *Stars* indicate significant difference between values obtained for *chlorina* mutant and the corresponding WT at $p<0.05$

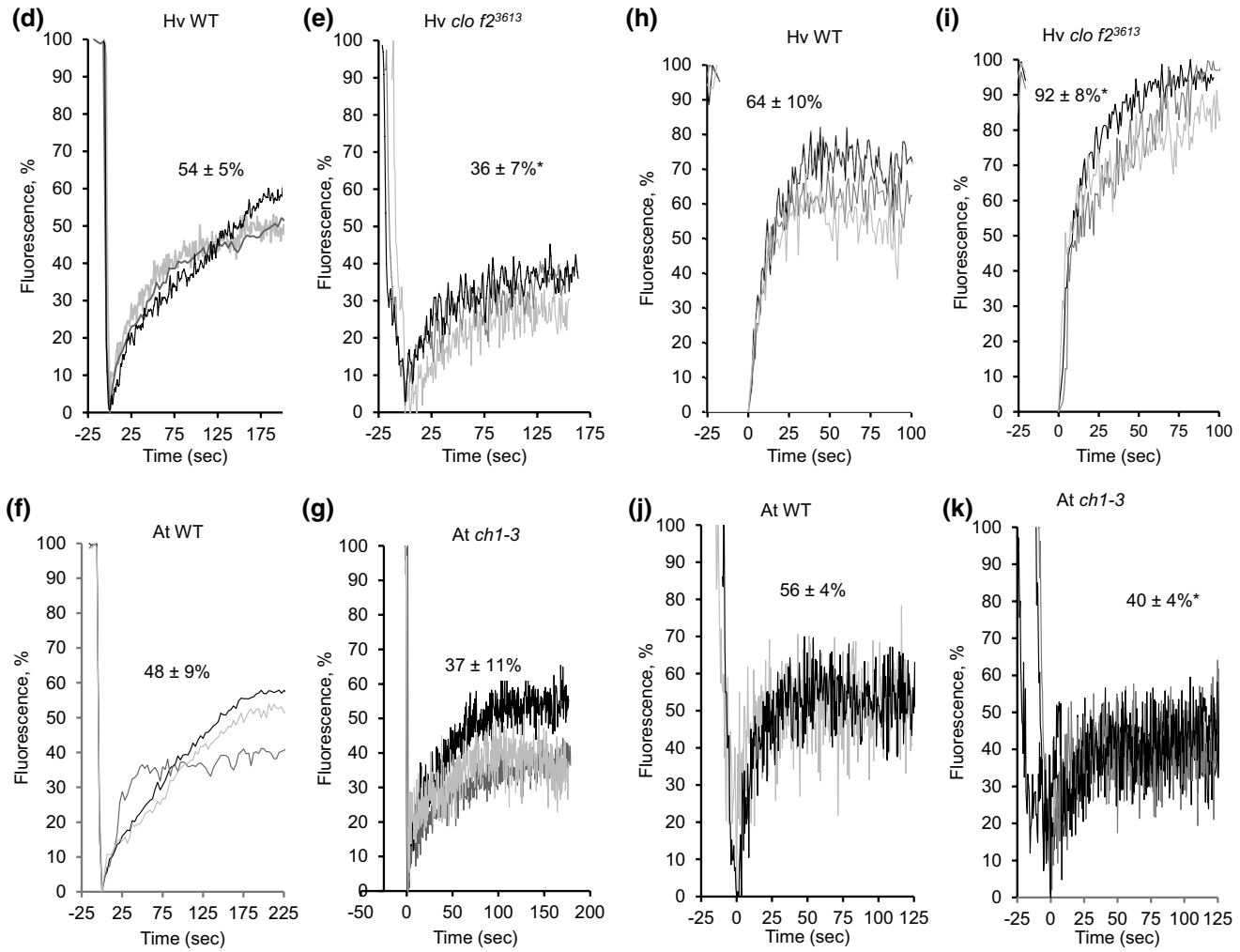

Fig. 1 (continued)

membranes. In Arabidopsis, the rates of BODIPY fluorescence recovery in WT and *ch1-3* mutant were significantly different (Fig. 1j, k) in that the fluorescence of the mobile fraction was lower in the membranes of *ch1-3*. Altogether, the data show that the diffusion of PSII complexes is significantly challenged in the membranes of barley *clo f2*^{3613}, but not in Arabidopsis *ch1-3* mutant, compared to membranes of the corresponding WT. The lateral mobility of lipids in thylakoid membranes of the barley *clo f2*^{3613} mutant was significantly higher, and that in the Arabidopsis *ch1-3* mutant significantly lower, than in WT membranes.

All LHC proteins are present in barley *clo f2*^{3613} leaves, but the levels of most of them are low

The different effects of the chlorophyll a oxygenase (CAO) mutation on lateral mobility of pigment–protein complexes in thylakoid membranes of barley *clo f2*^{3613} and Arabidopsis *ch1-3* mutants, respectively, could be related to the size and geometry of the complexes (de Bianchi et al. 2008; Goral et al. 2012). The composition of PSII antennae in the Arabidopsis *ch1-3* mutant has been analyzed (Kim et al. 2009). The levels of all Lhcb proteins, but especially those of Lhcb4 and Lhcb6, were significantly reduced compared to the WT except for the levels of Lhcb3 and Lhcb5 which were found to be similar and increased, respectively (Kim et al. 2009). As no information on the levels of LHC proteins has been published for the barley *clo f2*^{3613} mutant, immunoblots were performed (Fig. 2). They showed that the levels of most of LHC proteins in leaves of barley *clo f2*^{3613} were lower than in WT, although the level of decrease was different for each LHC protein. The most pronounced decrease was observed for Lhcb2, Lhcb4, Lhcb6, Lhca2, and Lhca4 proteins, while the levels of Lhca1, Lhca3, and Lhcb1 were much less affected, and those of Lhcb3 and Lhcb5 did not change at all in barley *clo f2*^{3613} (Fig. 2). In both Arabidopsis *ch1-3* and barley *clo f2*^{3613} mutants, no trimeric LHCBII was detected (Kim et al. 2009; our data

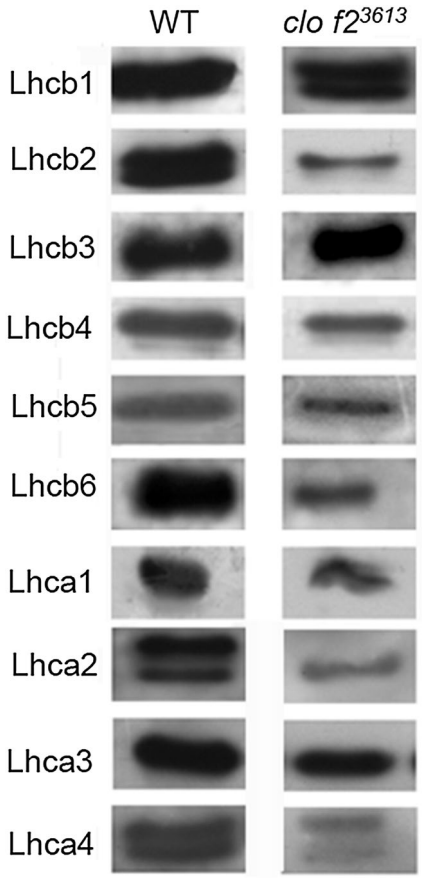

Fig. 2 Immunoblots of antennae proteins in barley leaves (WT and *clo f2*^{3613}). LDS membrane protein extracts containing 15 µg protein were loaded per lane

obtained by native gel electrophoreses, not shown). It can be concluded that at least in barley *clo f2*^{3613} plants grown as described in the "Materials and methods" section, the changes in Lhcb protein levels caused by the absence of functional CAO and the resulting lack of Chl*b* were similar to those observed in the Arabidopsis *ch1-3* mutant (Kim et al. 2009).

Under high light conditions, the PQ pool is more reduced in barley *clo f2*^{3613} leaves, but not in Arabidopsis *ch1-3* leaves, than in the corresponding WT leaves

As the size of mobile fraction of the BODIPY incorporated in the thylakoid membrane is an estimate of the lateral motility of lipids and low molecular weight membrane components (Tietze et al. 2015), the different values obtained for BODIPY fluorescence dynamics in thylakoid membranes of barley *clo f2*^{3613} and Arabidopsis *ch1-3* were indicative of the fact that the diffusion of low molecular weight molecules, such as PQ and xanthophylls, within the thylakoid membranes is facilitated in barley *clo f2*^{3613} but lowered in Arabidopsis *ch1-3*. The rates of PQ diffusion were suggested to represent a limiting step in PQ oxidation by Cyt b_6/f (Blackwell et al. 1994). To see whether the changes in lateral mobility of lipids in thylakoid membranes of *chlorina* mutants correlate with the redox state of the PQ pool, we first compared the sizes of PQ pools in leaves of barley and Arabidopsis WT and *chlorina* mutants as could be estimated from the areas above the fluorescence induction curves between F_o and F_m (Fig. 3a). No significant differences were observed. Under high light conditions (1500 µmol m^{-2} s^{-1} for 15 min), the PQ pool in barley *clo f2*^{3613} was significantly more reduced than in the corresponding WT (Fig. 3b). Under similar light conditions, Arabidopsis leaves of both WT and *ch1-3* showed a strong descrease in the F_v/F_m value (data not shown). Therefore,

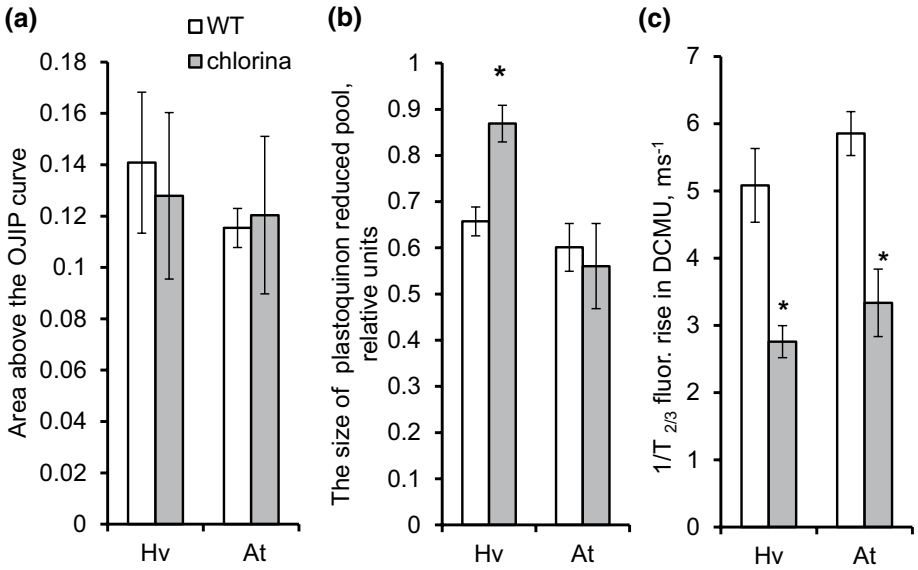

Fig. 3 Characteristics of antennae and PQ pool determined for leaves of Arabidopsis (At) and barley (Hv), WT and *chlorina* mutants (*ch1-3* and *clo f2*^{3613}, respectively): **a** size of total PQ pools determined as fully reduced PQ in DCMU-poisoned leaves; **b** size of pools of reduced PQ determined under high light (HL); **c** functional antenna size determined as 1/$T_{2/3}$ of the rise of Chl fluorescence during induction in leaves infiltrated with 200 µM DCMU. Each value is a mean of five (**a, b**) or ten (**c**) independent measurements ± SD. *Stars* indicate significant difference at $p < 0.05$ according to *t* test

the light intensity of 1000 µmol m^{-2} s^{-1} for 15 min was used to test the reduction of the PQ pool. No differences in the PQ reduction state were observed between leaves of Arabidopsis WT and *ch1-3* (Fig. 3b). The size of the functional antenna of PSII estimated from the time of fluorescence rise during fluorescence induction in DCMU-treated leaves was significantly decreased to nearly similar extents in both *chlorina* mutants relative to the corresponding WT (Fig. 3c), suggesting similar limitations of the light harvesting in the mutants. Further analyses of Chl fluorescence parameters obtained from fluorescence induction curves are shown in Table 1. A significant decrease in F_o, probably reflecting the smaller antennae, and a concomitant decrease in F_m were revealed for both *chlorina* mutants. The maximum quantum efficiency of PSII photochemistry (F_v/F_m) was similar in *chlorina* mutants and wild-type plants in both Arabidopsis and barley. In both *chlorina* mutants, the flux of absorbed energy per active PSII reaction center (RC)—ABS/RC—was significantly lower than in the corresponding WT. Quantum yield of electron transport from Q_A to Q_B in PSII (ET_{2o}/RC) was similar in WT and *clo f2*^{3613} barley mutant but was significantly lower in Arabidopsis *ch1-3* than in WT. Altogether, the data indicated that the PSII RC in both *chlorina* mutants received less energy than in the corresponding WT, obviously due to the fact that the antenna was reduced. However, while in Arabidopsis *ch1-3*, this did not lead to a change in the PQ pool reduction state as compared to the WT, in barley *clo f2*^{3613}, a similar limitation of light harvesting led to over-reduction of the PQ pool.

To analyze whether the lower ability to oxidize PQ in the barley *clo f2*^{3613} mutant compared to the WT can be due to changed stoichiometry of PSII and Cyt b_6/f proteins, immunoblots were performed and the relative amounts of the PsbA and PetA proteins were estimated (Fig. 3a, b). The ratios of PsbA/PetA were significantly increased in *clo f2*^{3613} compared to the WT, and were twice as high as the corresponding values in the WT, indicating a decrease in the amounts of Cyt b_6/f relative to PSII in the mutant (Fig. 3b). This indicates that a reason for a highly reduced state of the PQ pool in barley *clo f2*^{3613} mutant could well be a decrease in Cyt b_6/f amounts relative to PSII. The over-reduction of the PQ pool suggested that production of reactive oxygen species (ROS) is enhanced in leaves of barley *clo f2*^{3613} compared to the WT. To gain insight into the levels of different ROS in barley *clo f2*^{3613} and the WT, the leaves were infiltrated with ROS-sensitive dyes—either with a dye specific for singlet oxygen (SOSG) or with general ROS indicator (CM-H_2DCFDA)—and exposed for 2 h to high light. Analysis of fluorescence of the dyes after this period did not reveal any significant increase in singlet oxygen levels in *clo f2*^{3613} compared to the WT (Fig. 5a, b). However, fluorescence of CM-H_2DCFDA was strongly increased in leaves of *clo f2*^{3613} indicating that ROS levels were high after exposure to high light in the mutant, in contrast to the situation in WT leaves (Fig. 5c, d).

Table 1 Values of the basic chlorophyll fluorescence parameters derived from O–J–I–P tests for dark-adapted intact plants

Parameters	*Arabidopsis thaliana*		*Hordeum vulgare*	
	WT	*ch1-3*	WT	*clo f2*^{3613}
F_o	0.80 ± 0.18	0.47 ± 0.22*	0.49 ± 0.03	0.20 ± 0.02*
F_m	3.64 ± 0.21	1.98 ± 1.02*	2.05 ± 0.15	0.94 ± 0.11*
F_v/F_m	0.78 ± 0.04	0.76 ± 0.03	0.76 ± 0.02	0.78 ± 0.03
ABS/RC	6.21 ± 0.89	4.51 ± 0.30*	2.19 ± 0.33	1.65 ± 0.27*
ET_{2o}/RC	0.56 ± 0.06	0.44 ± 0.07*	0.45 ± 0.05	0.41 ± 0.02

Mean values ± SD are shown. Asterisks indicate significant difference at $p < 0.05$ according to *t* test

Structure of isolated grana membranes in field-grown barley WT and *clo f2*^{3613} plants

One of the factors affecting the lateral mobility of pigment–protein complexes and of the molecules of low molecular weight in grana membranes has been shown to be the organization of the complexes into ordered semi-crystalline arrays (Goral et al. 2012; Tietz et al. 2015). Such arrays had been observed in the grana membranes of chloroplasts of both WT and *chlorina f2* mutant of barley (Miller et al. 1976; Simpson 1978), but the packing density of particles in the semi-crystalline rows was twice as high in the mutant as in the WT (Miller et al. 1976). We analyzed the presence of the ordered rows of pigment–protein complexes in grana membranes isolated from leaves of barley WT and *clo f2*^{3613} plants grown outdoors, because these plants produced more leaves than greenhouse-grown barley. Figure 6 shows two examples of EM of negatively stained grana membranes obtained by partial solubilization with α-dodecylmaltoside for each barley WT and *clo f2*^{3613}, respectively Surprisingly, no major differences in the arrangement and size of the particles could be observed between barley WT and *clo f2*^{3613} (Fig. 6). In some grana membranes isolated from the WT, rows of ordered particles could be detected but such rows were never found in grana isolated from *clo f2*^{3613} leaves. The density of visible particles was somewhat higher in WT grana membranes (Fig. 6).

Discussion

The supramolecular level of organization of photosynthetic membranes has been revealed by recent studies as an important regulator of major processes of photosynthesis such as

transfer of energy and electrons, and also of repair of the D1 protein (reviewed by Kirchhoff 2014). This information has been gained from studies on chloroplasts obtained from spinach or Arabidopsis wild-type plants, but also from transgenic Arabidopsis lines lacking individual antenna proteins or other single components of the photosynthetic machinery like PsbS (de Bianchi et al. 2008, 2011; Haferkamp et al. 2010; Johnson et al. 2011; Goral et al. 2012; Kouril et al. 2013; Tietz et al. 2015). These studies have been extraordinarily useful in dissecting the role of the phenomenon of macromolecular crowding in photosynthetic membranes, using models where either none, or one or two components of photosynthetic machinery at once, were lacking. In the present study, we addressed for the first time the effects of supramolecular organization of grana membranes on photosynthetic characteristics in *chlorina* mutants of Arabidopsis and barley, respectively, where the absence of Chl*b* causes simultaneous changes in several components of pigment–protein complexes of PSII. We show that in spite of nearly similar reduction of antennae in both *chlorina* mutants, the effects on lateral mobility of pigment–protein complexes and lipids in grana membranes were different in both mutants. Also, the state of the PQ pool in both mutants did not correlate with the shift in the lateral mobility of lipids. This further highlights the complexity of the processes underlying the pleiotropic effects caused by mutations in the *CAO* gene in *chlorina* mutants of different plant species (reviewed in Voitsekhovskaja and Tyutereva 2015).

Strikingly, the sizes of the mobile fraction determined in our experiments for grana membranes of WT plants of barley as well as Arabidopsis for both lipids and Chl-containing proteins were considerably higher than the values reported by other studies. In the present study, the sizes of the mobile fractions for protein complexes were 48 ± 9% for Arabidopsis and 54 ± 5% for barley, respectively (Fig. 1f, d), while previous studies reported, e.g., for Arabidopsis WT, the values of 25% (Kirchhoff et al. 2008) and 18% (Tietz et al. 2015); and for spinach, 15% (Goral et al. 2010) and 13% (Johnson et al. 2011). The size of mobile fractions determined for lipids was 56 ± 4% for Arabidopsis and 64 ± 10% for barley, respectively (Fig. 1j, h). The corresponding value reported for Arabidopsis WT was 26% (Tietz et al. 2015). An increase in protein mobility was demonstrated in intact chloroplasts subjected to photoinhibitory treatment which depended on STN7 and STN8 protein kinases, indicating that LHCII complexes are involved (Goral et al. 2010). However, the sizes of mobile fractions in *chlorina* mutants lacking the mobile trimeric LHCII antenna were in a range similar to those in the corresponding WT (Fig. 1e, g). Therefore, it seems unlikely that the observed values were due to photoinhibition of chloroplasts of WT plants in our experiments. Rather, the differences between the previously published values and the values observed in this study are likely to be related to the different bleaching approaches applied. We noticed that severe bleaching of Chl fluorescence down to 0 often led to a rapid increase of fluorescence during the first seconds of recovery but then the increase stopped and, after a period of steady-state, a loss of fluorescence occurred in the bleached stripe (data not shown). For these trials, calculation returned very low values of mobile fraction sizes which we ascribed to irreversible changes in the thylakoid membranes of intact chloroplasts. However, when Chl fluorescence was bleached down to only 50% of the initial level, the recovery phase was stable and in most cases, recovery to 80% and more took place over a time of more than 10 min (data not shown). Also, in our experiments, 100% intensity of the 405 nm laser was used for bleaching, while other studies used an increase in the 488 nm laser power by a factor of 32 for the same purpose (Kirchhoff et al. 2008; Johnson et al. 2011). We propose that the higher values for protein and lipids mobility observed with less severe bleaching are closer to the in vivo situation.

In barley *clo f2*^{3613}, the size of the mobile fraction of Chl-containing protein complexes, which in *chlorina* mutants do not include LHCII trimers (Miller et al. 1976; Simpson 1978; Kim et al. 2009) but only PSII RC with attached Lhcb proteins was lower than in the WT (Fig. 1d, e). At the same time, no significant changes were detected between the mobile fractions of Chl-containing proteins of Arabidopsis WT and *ch1-3* (Fig. 1f, g). Notably, the fluctuations of Chl fluorescence during the recovery phase were much more pronounced in both *chlorina* mutants than in the corresponding WT (Fig. 1d, f compared to Fig. 1e, g). We speculate that the range of fluctuations might be related to the size of Chl-containing protein complexes which are expected to be smaller in both *chlorina* mutants due to the lowered levels of most antenna proteins (Kim et al. 2009; Fig. 2) but the elucidation of the nature of those fluctuations requires additional studies.

The size of the mobile fractions of lipids in barley *clo f2*^{3613} was considerably higher than that in the WT (Fig. 1h, i). This fact, together with the significant decrease of the size of the mobile protein fraction, suggests the presence of semi-crystalline rows in the grana membranes of the barley *clo f2*^{3613} mutant. Tietz et al. (2015) have demonstrated that the formation of such rows in grana membranes of Arabidopsis *fad5* mutant led to a decrease in the lateral mobility of proteins and a concomitant increase in lipid mobility. A high rate of formation of semi-crystalline rows has been reported repeatedly for barley *chlorina f2* mutants (e.g., Miller et al. 1976; Simpson 1978). To the best of our knowledge, the presence of such rows in Arabidopsis *chlorina* mutants had never been analyzed but could well be expected. However, the comparison of the sizes of the

mobile fractions of lipids and Chl-containing proteins for Arabidopsis WT and *ch1-3* do not support this assumption for the plants used in our experiments, as the lateral mobility of lipids was decreased, not increased, in the mutant, and no changes at all were found for Chl-containing proteins (Fig. 1 f, g, j, k).

The observed rise in lateral mobility of lipids in grana membranes of barley *clo f2*^{3613} suggested that the diffusion of PQ would be facilitated, preventing an over-reduction of the PQ pool. Similarly, the significant decrease in the lateral mobility of lipids in Arabidopsis *ch1-3* suggested the opposite. However, this was not confirmed by analyses of Chl fluorescence transients in leaves of barley and Arabidopsis. Although the sizes of the PQ pool were nearly equal in all WT and *chlorina* mutants studied (Fig. 3a), and the decrease in the functional antenna size was similar for both *chlorina* mutants compared to the corresponding WT (Fig. 3c; Table 1), the PQ pool in the light was over-reduced in barley *clo f2*^{3613} as compared to the corresponding WT while in Arabidopsis, the reduction state of the PQ pool was similar in WT and *ch1-3* (Fig. 3b). For Arabidopsis, a decrease in the quantum yield of electron transport from Q_A to Q_B in *ch1-3* compared to the WT (Table 1) suggested a decrease in the electron flow from PSII to PQ. Obviously, the limitations of PQ diffusion suggested by the FRAP analyses compensated for the effect of this decreased electron flow on the redox state of the PQ pool. For barley, the quantum yield of electron flow from Q_A to Q_B in PSII was similar for *clo f2*^{3613} and WT (Table 1). Here, the over-reduction of the PQ pool in *clo f2*^{3613} compared to the WT observed in spite of the decrease in energy input from the antenna to PSII cannot be explained without further experimentation. However, the analyses of the levels of PsbA and PetA proteins showed a twofold increase in the levels of PSII relative to Cytb$_6$/f which can account for a higher supply of electrons to the PQ pool which could not be effectively accepted by Cytb$_6$/f in spite of the increase of PQ diffusion suggested by FRAP analyses performed on *clo f2*^{3613} (Fig. 4). We propose that the changed stoichiometry of PSII relative to Cytb$_6$/f is a reason for the over-reduction of the PQ pool in barley *clo f2*^{3613}. The increase in lipid lateral mobility in barley *clo f2*^{3613} could be interpreted as a compensatory reaction to the low mobility of PSII complexes facilitating their repair (Allakhverdiev and Murata 2004; Kreslavski et al. 2007; Kirchhoff 2014). At the same time, the decrease in lipid lateral mobility in Arabidopsis *ch1-3* could be seen as a compensatory reaction to prevent high oxidation of the PQ pool caused by lowered quantum yield of electron transfer within PSII. Further study of the lipid composition of thylakoid membranes in *chlorina* mutants would help understand these phenomena (Los et al. 2013).

The increase in CM-H_2DCFDA fluorescence in *clo f2*^{3613} compared to the corresponding WT (Fig. 5c, d)

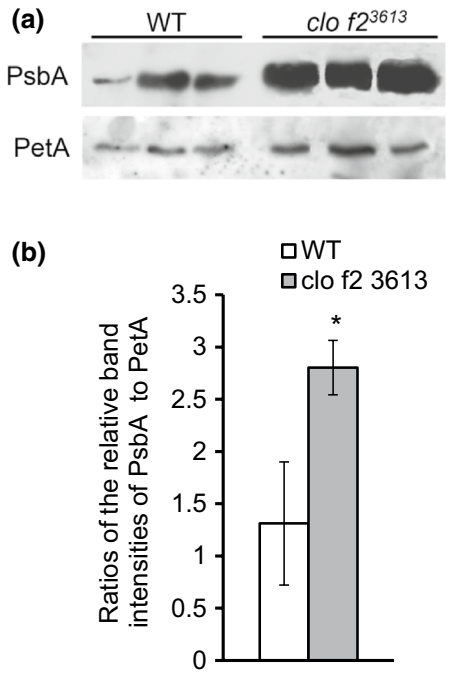

Fig. 4 Relative amounts of Cyt b_6/f per PSII RC as determined by immunoblots of LDS membrane protein extracts obtained from barley leaves (WT and *clo f2*^{3613}). **a** Examples of immunoblots of PetA and PsbA proteins. LDS membrane protein extracts corresponding to 10 µg protein were loaded per lane. **b** Ratios of the relative intensities of bands obtained with anti-PetA and anti-PsbA antibodies as shown in **a**, corresponding to Cyt b_6/f/PSII RC. Means ± SD for three (WT) or five (*clo f2*^{3613}) independent samples are shown

probably reflects the enhanced production of H_2O_2 and superoxide from over-reduced PQ within grana membranes of *clo f2*^{3613}: it has been demonstrated that the initial stage of O_2 reduction in PQ pool is generation of superoxide by semiplastoquinone (Khorobrykh and Ivanov 2002) which is rapidly reduced to H_2O_2 in the presence of high amounts of PQH_2 (Ivanov et al. 2017). Although it might be speculated that H_2O_2 and other ROS would have some destructive effects on photosynthetic machinery, this was obviously not the case as the F_v/F_m value did not change in leaves of the mutant compared to the WT. Similarly, no decrease of F_v/F_m was observed in Arabidopsis leaves exposed to H_2O_2 in the concentration range of 50–100 mM for several days (B.N. Ivanov, M.M. Borisova-Mubarakshina, D.V. Vetoshkina, personal communication). Surprisingly, we could not detect any significant increase in singlet oxygen levels in *clo f2*^{3613} compared to the WT (Fig. 5a, b), which is in accordance with the fact that the levels of electron transport from Q_A to Q_B in PSII did not differ significantly (Table 1). The main source of singlet oxygen in leaves is the energy transfer reactions from the excited triplet state of Chl to molecular oxygen, and the level of triplet state formation increases when electron transfer from

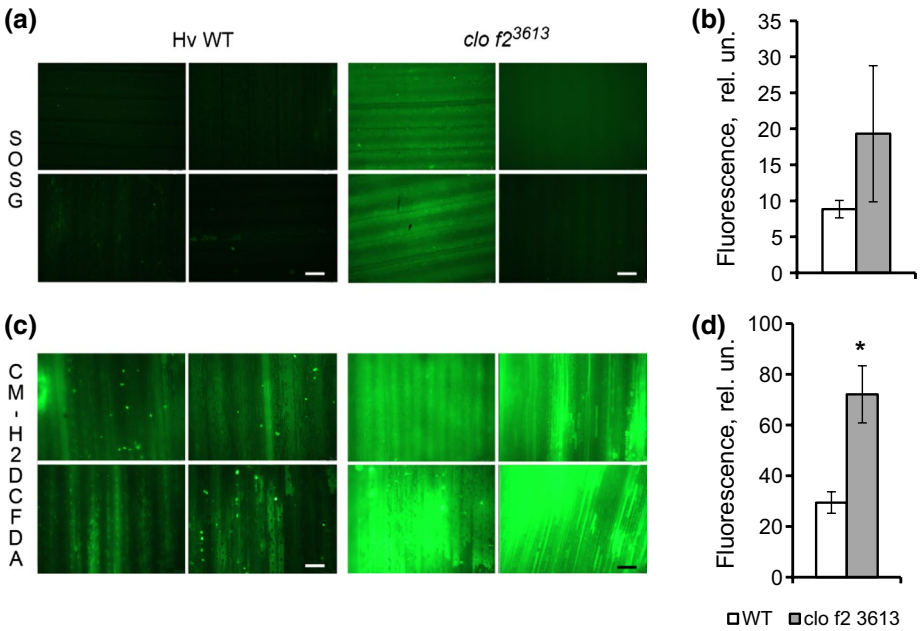

Fig. 5 Fluorescence of singlet oxygen sensor green (SOSG) (**a, b**) and of CM-H_2DCFDA (**c, d**) determined in barley leaves (WT and *clo f2*^{3613}). **a** Representative fluorescent images of SOSG-infiltrated leaves after 2-h exposure to high hight; **b** quantitative estimation of ROS production; **c** representative fluorescent images of CM-H_2DCFDA-infiltrated leaves after 2-h exposure to high hight; **d** quantitative estimation of ROS production. Each value represents a mean ± SD of five to ten independent biological samples (**b, d**). *Scale bar* 20 µm

Q_A to Q_B is hindered (Krieger-Liszkay 2005). Formation of singlet oxygen has been reported for an allelic Arabidopsis *ch1-1* mutant (Ramel et al. 2013); we also observed it in mature barley *clo f2*^{3613} plants grown in the field using SOSG staining (Dmitrieva et al. 2017).

The formation of semi-crystalline rows in grana membranes has been shown to represent a dynamic parameter affected both in isolated chloroplasts and in vivo by environmental factors such as light or temperature in a time scale of a few hours (Semenova 1995; Johnson et al. 2011). The formation of such rows is well established for barley *chlorina f2* mutants (e.g., Miller et al. 1976; Simpson 1978), and in our study was suggested to have occurred based on changes in protein and lipid mobility determined in grana membranes of barley *clo f2*^{3613} by FRAP analyses. Therefore, we were surprised that we failed to detect such rows in *clo f2*^{3613}, although patches of semi-crystalline arrays could be visualized in some grana of WT chloroplasts (Fig. 6). The developmental stage of barley *clo f2*^{3613} plants used for isolation of grana membranes was similar to that in other studies (Miller et al. 1976; Simpson 1978). The most probable reason is the light conditions at which the *clo f2*^{3613} plants in our study were grown for different analyses. Only the plants used for EM analyses of grana were grown in the field, where plants regularly experience PPFR of 1500 µmol m^{-2} s^{-1} and more, while the plants used for the FRAP analyses were grown in a greenhouse during autumn where PPFR did not exceed 800 µmol m^{-2} s^{-1} on sunny days. The latter conditions are close those used by Miller et al. (1976) and Simpson (1978). In accordance to this, Kouril et al. (2013) found that the frequency of formation of semi-crystalline rows in Arabidopsis WT plants was drastically reduced by plants' exposure to high light. Altogether, the data support the hypothesis that the supramolecular organization of photosynthetic complexes in grana membranes is a highly dynamic parameter which influences, and is itself influenced, by multiple environmental and endogenous factors.

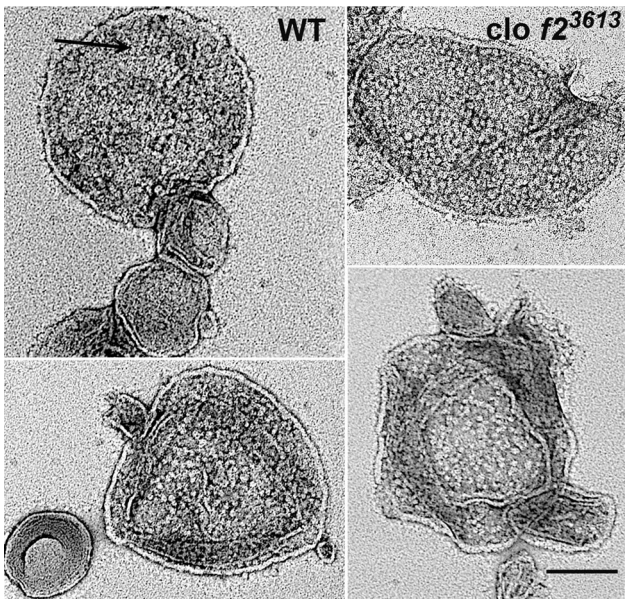

Fig. 6 EM of negatively stained grana membranes of chloroplasts of barley plants (WT and *clo f2*^{3613}) grown outdoors. Partially solubilized grana membranes were obtained using 0.2% α-dodecylmaltoside. *Arrow* points on a membrane patch with ordered particles. *Scale bar* 100 nm

In conclusion, this study has demonstrated that lateral mobility of PSII complexes and lipids in grana membranes of chloroplasts of *chlorina* mutants of Arabidopsis and barley is differently affected in spite of nearly similar changes of antennae. We propose that the size of the mobile fractions of Chl proteins in grana membranes in vivo might be higher than reported previously. The study of *chlorina* mutants has demonstrated that the effects exerted by alterations in the supramolecular organization of grana membranes on photosynthetic processes can in some cases be compensated by other factors, and the resulting phenotype cannot be predicted based alone on the diffusion parameters of Chl proteins and lipids in grana membranes.

Acknowledgements This paper is dedicated to the memory of Prof. em. Dr. Ulrich Heber (1930–2016). We thank Dr. Tomas Morosinotto (University of Padova, Italy) for kindly sharing with us the protocol of grana isolation. We are grateful to Ms Valeria A. Dmitrieva for help with some experiments and to Dr. Boris N. Ivanov for sharing unpublished results. This study was supported by the Russian Science Foundation (project #14-16-00120 to OVV). The Core Facilities Center "Cell and Molecular Technologies in Plant Science" at the Komarov Botanical Institute RAS (Saint-Petersburg, Russia) and the Research Resource Centre for Molecular and Cell Technologies of Saint-Petersburg State University are gratefully acknowledged for technical support.

References

Allakhverdiev SI, Murata N (2004) Environmental stress inhibits the synthesis de novo of proteins involved in the photodamage-repair cycle of photosystem II in *Synechocystis* sp. PCC 6803. Biochim Biophys Acta 1657:23–32

Apel P (1967) Photosynthesemessungen an Chlorophyllmutanten von Gerste (Lichtkurven, "light-Atmung", Starklichtemfindlichkeit). Stud Biophys 5:105–110

Arnon D (1949) Copper enzymes in isolated chloroplasts: polyphenoloxidase in *Beta vulgaris*. Plant Physiol 24:1–15

Bassi R, Hinz U, Barbato R (1985) The role of the light harvesting complex and photosystem II in thylakoid stacking in the *chlorina-f2* barley mutant. Carlsberg Res Commun 50:347–367

Blackwell MF, Gibas C, Gygax S, Roman D, Wagner B (1994) The plastoquinone diffusion coefficient in chloroplasts and its mechanistic implications. Biochim Biophys Acta 1183:533–543

Borisova-Mubarakshina MM, Ivanov BN, Vetoshkina DV, Lubimov VY, Fedorchuk TP, Naydov IA, Kozuleva MA, Rudenko NN, Dall'Osto La, Cazzaniga S, Bassi R (2015) Long-term acclimatory response to excess excitation energy: evidence for a role of hydrogen peroxide in the regulation of photosystem II antenna size. J Exp Bot 66:7151–7164

Bossmann BL, Knoetzel J, Jansson S (1997) Screening of *chlorina* mutants of barley (*Hordeum vulgare* L.) with antibodies against light-harvesting proteins of PS I and PS II: absence of specific antenna proteins. Photosynth Res 52:127–136

Bossmann BL, Grimme H, Knoetzel J (1999) Protease-stable integration of Lhcb1 into thylakoid membranes is dependent on chlorophyll b in allelic chlorina-f2 mutants of barley (*Hordeum vulgare* L). Planta 207:551–558

Brestic M, Zivcak M (2013) PSII Fluorescence techniques for measurement of drought and high temperature stress signal in crop plants: protocols and applications. In: Rout GR, Das AB (eds) Molecular stress physiology of plants. Springer, Dordrecht, pp 87–131

de Bianchi S, Dall'Osto L, Tognon G, Morosinotto T, Bassi R (2008) Minor antenna proteins CP24 and CP26 affect the interactions between photosystem II subunits and the electron transport rate in grana membranes of Arabidopsis. Plant Cell 20:1012–1028

de Bianchi S, Betterle N, Kouril R, Cazzaniga S, Boekema E, Bassi R, Dall'Osto L (2011) Arabidopsis mutants deleted in the light-harvesting protein Lhcb4 have a disrupted photosystem II macrostructure and are defective in photoprotection. Plant Cell 23:2659–2679

Dmitrieva VA, Ivanova AN, Tyutereva EV, Evkaikina AI, Klimova EA, Voitsekhovskaja OV (2017) Chlorophyllide-a-Oxygenase (CAO) deficiency affects the levels of singlet oxygen and formation of plasmodesmata in leaves and shoot apical meristems of barley. Plant Signal Behav. doi:10.1080/15592324.2017.1300732

Dulin D, Le Gall A, Perronet K, Soler N, Fourmy D, Yoshizawa S, Bouyer P, Westbrook N (2010) Reduced photobleaching of BODIPY-FL. Phys Proc 3:1563–1567

Espineda CE, Alicia SL, Domenica D, Brusslan JA (1999) The AtCAO gene, encoding chlorophyll a oxygenase, is required for chlorophyll b. Proc Natl Acad Sci USA 96:10507–10511

Goral TK, Johnson MP, Brain APR, Kirchhoff H, Ruban AV, Mullineaux CW (2010) Visualizing the mobility and distribution of chlorophyll proteins in higher plant thylakoid membranes: effects of photoinhibition and protein phosphorylation. Plant J 62:948–959

Goral TK, Johnson MP, Duffy CDP, Brain APR, Ruban AV, Mullineaux CW (2012) Light-harvesting antenna composition controls the macrostructure and dynamics of thylakoid membranes in Arabidopsis. Plant J 69:289–301

Haferkamp S, Haase W, Pascal AA, van Amerongen H, Kirchhoff H (2010) Efficient light harvesting by photosystem II requires an optimized protein packing density in grana thylakoids. J Biol Chem 108:17020–17028

Härtel H, Lokstein H, Grimm B, Rank B (1996) Kinetic studies on the xanthophyll cycle in barley leaves (Influence of antenna size and relations to nonphotochemical chlorophyll fluorescence quenching). Plant Physiol 110:471–482

Havaux M, Dall'osto L, Bassi R (2007) Zeaxanthin has enhanced antioxidant capacity with respect to all other xanthophylls in Arabidopsis leaves and functions independent of binding to PSII antennae. Plant Physiol 145:1506–1520

Highkin HR, Frenkel AW (1962) Studies of growth and metabolism of a barley mutant lacking chlorophyll b. Plant Physiol 37:814-820

Ivanov AG, Allakhverdiev SI, Huner NP, Murata N (2012) Genetic decrease in fatty acid unsaturation of phosphatidylglycerol increased photoinhibition of photosystem I at low temperature in tobacco leaves. Biochim Biophys Acta 1817:1374–1379

Ivanov BN, Borisova-Mubarakshina MM, Kozuleva MA (2017) Formation mechanisms of superoxide radical and hydrogen peroxide in chloroplasts, and factors determining the signaling by hydrogen peroxide. Funct Plant Biology. doi:10.1071/FP16322

Johnson M, Goral TK, Duffy CDP, Brain APR, Mullineaux CW, Ruban AV (2011) Photoprotective energy dissipation involves the reorganization of photosystem II light-harvesting complexes in the grana membranes of spinach chloroplasts. Plant Cell 23:1468–1479

Johnson M, Vasilev C, Olsen JD, Hunter CN (2014) Nanodomains of cytochrome b6f and photosystem II complexes in spinach grana thylakoid membranes. Plant Cell 26:3051–3061

Kalaji HM, Schansker G, Ladle RJ, Goltsev V, Bosa K, Allakhverdiev SI, Brestic M, Bussotti F, Calatayud A, Dabrowski P, Elsheery NI, Ferroni L, Guidi L, Hogewoning SW, Jajoo A,

Misra AN, Nebauer SG, Pancaldi S, Penella C, Poli D, Pollastrini M, Romanowska-Duda ZB, Rutkowska B, Serodio J, Suresh K, Szulc W, Tambussi E, Yanniccari M, Zivcak M (2014) Frequently asked questions about in vivo chlorophyll fluorescence: practical issues. Photosynth Res 122:121–158

Khorobrykh SA, Ivanov BN (2002) Oxygen reduction in a plastoquinone pool of isolated pea thylakoids. Photosynth Res 71:209–219

Kim EH, Li XP, Razeghifard R, Anderson JM, Niyogi KK, Pogson BJ, Chow WS (2009) The multiple roles of light-harvesting chlorophyll a/b-protein complexes define structure and optimize function of Arabidopsis chloroplasts: a study using two chlorophyll b-less mutants. Biochim Biophys Acta 1787:973–984

Kirchhoff H (2013) Architectural switches in plant thylakoid membranes. Photosynth Res 116:481–487

Kirchhoff H (2014) Diffusion of molecules and macromolecules in thylakoid membranes. Biochim Biophys Acta 1837:495–502

Kirchhoff H, Horstmann S, Weis E (2000) Control of the photosynthetic electron transport by PQ diffusion microdomains in thylakoids of higher plants. Biochim Biophys Acta 1459:148–168

Kirchhoff H, Mukherjeei U, Galla H-J (2002) Molecular architecture of the thylakoid membrane: lipid diffusion space for plastoquinone. Biochemisrty 41:4872–4882

Kirchhoff H, Haferkamp S, Allen JF, Epstein DBA, Mullineaux CW (2008) Protein diffusion and macromolecular crowding in thylakoid membranes. Plant Physiol 146:1571–1578

Kouril R, Wientjes E, Bultema JB, Croce R, Boekema EJ (2013) High-light vs low-light: Effect of light acclimation on photosystem II composition and organization in Arabidopsis thaliana. Biochym Biophys Acta 1827:411-419

Kramer DM, Johnson G, Kiirats O, Edwards GE (2004) New fluorescence parameters for the determination of Q_A redox state and excitation energy fluxes. Photosynth Res 79:209–218

Kreslavski V, Carpentier R, Klimov V, Murata N, Allakhverdiev S (2007) Molecular mechanisms of stress resistance of the photosynthetic apparatus. Biochem (Mosc) Suppl Ser A 1:185–205

Krieger-Liszkay A (2005) Singlet oxygen production in photosynthesis. J Exp Bot 56:337–346

Kunugi M, Satoh S, Ihara K, Shibata K, Yamagishi Y, Kogame K, Obokata J, Takabayashi A, Tanaka A (2016) Evolution of green plants accompanied changes in light-harvesting systems. Plant Cell Physiol 57:1231–1243

Lavergne J, Bouchaud J-P, Joliot P (1992) Plastoquinone compartmentation in chloroplasts. II theoretical aspects. Biochim Biophys Acta 1101:13–22

Leverenz JW, Öquist G, Winglse G (1992) Photosynthesis and photoinhibition in leaves of chlorophyll b-less barley in relation to absorbed light. Physiol Plant 85:495–502

Lin Z-F, Lin G-Z, Peng C-L (2009) Enhancement of susceptivity to photoinhibition and photooxidation in rice chlorophyll b-less mutants. Photosynthetica 47:46–54

Los DA, Mironov KS, Allakhverdiev SI (2013) Regulatory role of membrane fluidity in gene expression and physiological functions. Photosynth Res 116:489–509

Miller KR, Miller GJ, McIntyre KR (1976) The light-harvesting chlorophyll-protein complex of photosystem II Its location in the photosynthetic membrane. J Cell Biol 71:624–638

Morosinotto T, Bassi R, Frigerio S, Finazzi G, Morris E, Barber J (2006) Biochemical and structural analyses of a higher plant photosystem II supercomplex of a photosystem I-less mutant of barley consequences of a chronic over-reduction of the plastoquinone pool. FEBS J 273:4616–4630

Mueller AH, Dockter C, Gough SP, Lundqvist U, von Wettstein D, Hansson M (2012) Characterization of mutations in barley fch2 encoding chlorophyllide a oxygenase. Plant Cell Physiol 53:1232–1246

Murashige T, Skoog F (1962) A revised medium for rapid growth and bio assays with tobacco tissue cultures. Physiol Plant 15:473–497

Murata N, Takahashi S, Nishiyama Y, Allakhverdiev SI (2007) Photoinhibition of photosystem II under environmental stress. Biochim Biophys Acta 1767:414–421

Nishiyama Y, Allakhverdiev SI, Murata N (2005) Inhibition of the repair of photosystem II by oxidative stress in cyanobacteria. Photosynth Res 84:1–7

Ramel F, Ksas B, Akkari E, Mialoundama AS, Monnet F, Krieger-Liszkay A et al (2013) Light-induced acclimation of the arabidopsis chlorina1 mutant to singlet oxygen. Plant Cell 25:1445–1462

Reits EA, Neefjes JJ (2001) From fixed to FRAP: measuring protein mobility and activity in living cells. Nat Cell Biol 3(6):E145–E147

Sagromsky H (1974) Zur physiologischen Bedeutung von Chlorophyll b. Biochem Physiol Pflanzen 166:95-104

Schmitt FJ, Renger G, Friedrich T, Kreslavski VD, Zharmukhamedov SK, Los DA, Kuznetsov VV, Allakhverdiev SI (2014) Reactive oxygen species: re-evaluation of generation, monitoring and role in stress-signaling in phototrophic organisms. Biochim Biophys Acta 1837:835–848

Semenova GA (1995) Particle regularity on thylakoid fracture faces is influenced by storage-conditions. Can J Bot 73:1676–1682. doi:10.1139/b95-181

Simpson DJ (1978) Freeze-fracture studies on barley plastid membranes II Wild-type chloroplasts. Carlsberg Res Commun 43:365–389

Standfuss J, Terwisscha van Scheltinga AC, Lamborghini M, Kühlbrandt W (2005) Mechanisms of photoprotection and nonphotochemical quenching in pea light-harvesting complex at 2.5 A resolution. EMBO J 24:919–928

Strasser RJ, Srivastava A, Tsimilli-Michael M (2000) The fluorescence transient as a tool to characterize and screen photosynthetic samples. In: Yunus M, Pathre U, Mohanty P (eds) Probing photosynthesis: mechanism, regulation and adaptation. Taylor & Francis, London

Strasser RJ, Srivastava A, Tsimilli-Michael M (2004) Analysis of the chlorophyll a fluorescence transient, advances in photosynthesis and respiration. In: Papageorgiou GC, Govindjee (eds) Chlorophyll fluorescence: a signature of photosynthesis. Kluwer Academic, Dordrecht

Takabayashi A, Kurihara K, Kuwano M, Kasahara Y, Tanaka R, Tanaka A (2011) The oligomeric states of the photosystems and the light-harvesting complexes in the Chl *b*-less mutant. Plant Cell Physiol 52:2103–2114

Tanaka R, Tanaka A (2011) Chlorophyll cycle regulates the construction and destruction of the light-harvesting complexes. Biochim Biophys Acta 1807:968–976

Tietz S, Puthiyaveetil S, Enlow HM, Yarbrough R, Wood M, Semchonok DA et al (2015) Functional implications of photosystem II crystal formation in photosynthetic membranes. J Biol Chem 290:14091–14106

Tremmel I, Kirchhoff H, Weis E, Farquhar CD (2003) Dependence of plastoquinol diffusion on the shape, size, and density of integral thylakoid proteins. Biochym Biophys Acta 1607:97–109

Tyutereva EV, Voitsekhovskaja OV (2011) Responses of chlorophyll *b*-less *chlorina 3613* barley mutant to a prolonged decrease in illuminance: 1. Dynamics of chlorophyll content, growth, and productivity. Russ J Plant Physiol 58:1–8

Voitsekhovskaja OV, Tyutereva EV (2015) Chlorophyll b in angiosperms: functions in photosynthesis, signaling and ontogenetic regulation. J Plant Physiol 189:51–64

Whitehouse DG, Moore AL (1993) Isolation and purification of functionally intact chloroplasts from leaf tissue and leaf tissue protoplasts. In: Graham JM, Higgins JA (eds) Methods in molecular biology, vol. 19: biomembrane protocols: I. Isolation and analysis. Humana Press, Totowa, pp 123–151